Trapping and guiding of acoustic waves by defect modes in a full-band-gap ultrasonic crystal

A. Khelif,[1] A. Choujaa,[1] B. Djafari-Rouhani,[2] M. Wilm,[1] S. Ballandras,[1] and V. Laude[1]
[1]*Laboratoire de Physique et Métrologie des Oscillateurs, CNRS UPR 3203, associé à l'Université de Franche-Comté, 32 avenue de l'Observatoire, 25044 Besançon cedex, France*
[2]*Laboratoire de Dynamique et Structures des Matériaux Moléculaires, CNRS UMR 8034, Université de Lille I, 59655 Villeneuve d'ascq cedex, France*
(Received 30 June 2003; published 5 December 2003)

We report on the experimental observation of the existence and the interaction of localized defect modes in a full acoustic band gap in a two-dimensional lattice of steel cylinders immersed in water. The confinement of defect modes and the splitting of their resonance frequencies are observed and are explained by their evanescent coupling. A different type of waveguiding in a phononic crystal based on the evanescent coupling of defect modes is proposed and demonstrated experimentally. The finite-difference time-domain method is used to interpret the experimental data and it is found that theoretical predictions properly account for the observed spectra.

DOI: 10.1103/PhysRevB.68.214301 PACS number(s): 43.20.+g, 43.40.+s, 46.40.Cd, 63.20.−e

The elastic analogs of photonic band-gap materials have received increasing attention recently. In spite of the analogy, the so-called elastic band-gap materials need further developments in light of their potential applications in a wide range of technologies. Elastic band gap materials, also termed phononic crystals, are inhomogeneous elastic media composed of one-, two-, or three-dimensional periodic arrays of inclusions embedded in a matrix. Several classes of phononic crystals exist and differ mainly by the physical nature of the inclusion and of the matrix. Among them, solid/solid, fluid/fluid, and mixed solid/fluid composite systems have received attention. These composite media typically exhibit stop bands in their transmission spectra for which the propagation of sound or vibration is strictly forbidden in all directions.[1–7] The location and the width of acoustic band gaps result from a large contrast in the value of the elastic constants and/or the mass density of the constitutive materials. By breaking the periodicity of the phononic crystal, it is possible to create highly localized defect or guided modes within the acoustic band gap, which are analogous to localized modes in photonic crystal[8] and to localized impurity states in a semiconductor.[9] This makes these systems potential candidates for the design of elastic or acoustic waveguides or filters.

In the case of solid/solid phononic crystals, the existence of full band gaps and localized defect modes and the possibility of guiding waves have been investigated theoretically.[10–12] In the case of fluid inclusions in a solid matrix, Torres *et al.* have shown experimentally the existence of full band gaps and have also investigated the possibility of guiding waves.[13] Cervera *et al.* have investigated the case of solid inclusions in a fluid matrix by low-frequency sonic experiments in air. They have experimentally observed full band gaps and demonstrated the principle of a phononic crystal acoustic lens.[14] The three-dimensional array of close-packed tungsten carbide beads in water investigated by Yang *et al.* is also of the solid inclusions-fluid matrix type and shows a full band gap through which tunneling was observed.[15]

In this paper, we investigate experimentally the acoustic band-gap effect in a 2D phononic crystal consisting of steel cylinders immersed in water. We report on the observation of the full band gap and of localized cavity or defect modes in the band gap that are introduced by removing one or more cylinders from the lattice. The effect of the coupling of defect modes on the splitting of their eigenmode or resonance frequencies is investigated. This effect is used to achieve a different type of waveguiding through evanescently coupled localized defects arranged in line. Measured data are compared with theoretical calculations of the spectra. Our calculations are based on a finite-difference time-domain (FDTD) method which has been recently used in several papers dealing with phononic crystals.[6,7,10–12] Let us recall that the supercell method, which in principle provides the dispersion curves, is not suitable for calculating the acoustic band structure of phononic crystals containing both solid and fluid components.[6,10]

We manufactured the 2D lattice by clamping 150-mm-long steel cylinders into a rigid periodically perforated steel plate. The cylinders have a diameter $d=2.5$ mm. The period of the square lattice is $a=3$ mm. This results in a filling fraction $F=\pi d^2/(4a^2)$ of approximately 55%. The choice of steel and water as the composite materials is based on the strong contrast in their densities and elastic constants. The experimental setup is based on the well-known ultrasonic immersion transmission technique, depicted in Fig. 1. In this technique, a couple of wide-bandwidth transmitter/receiver acoustic transducers operating around 450 kHz and with a diameter of 25 mm (Panametrics immersion transducers type Videoscan V301) are used. A pulser/receiver generator (Panametrics model 5800) produces a short duration (about 4 μs) pulse which is applied to the source transducer launching the probing longitudinal waves. The signal detected by the receiving transducer aligned with the source transducer is acquired by the pulser/receiver, post amplified, and then digitized by a digital sampling oscilloscope with a temporal resolution of 2.5 ns. To reduce random errors, 500 measurements are averaged before a fast Fourier transform is performed to obtain the transmission spectrum. The system

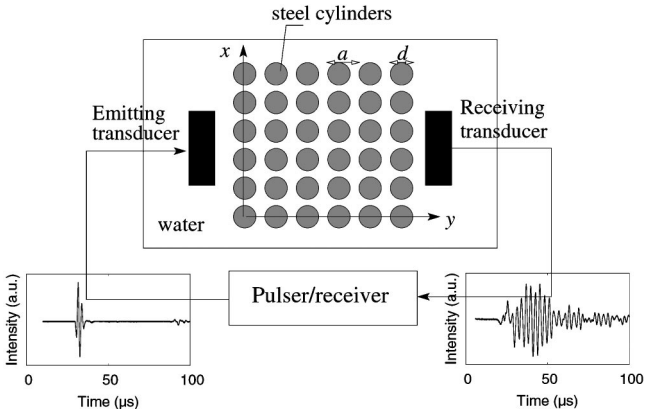

FIG. 1. Experimental setup used to measure the transmission spectra of phononic crystals using acoustic transducers immersed in water.

is first calibrated with no sample present; a reference signal is digitized and its spectrum is used to normalize the subsequent transmission spectra.

The effect of the direction of propagation on the band gaps was first evaluated by performing two transmission measurements through the perfect phononic crystal arranged such that the lattice thickness is either parallel to the ΓX or the ΓM directions of the square lattice Brillouin zone, as depicted in Fig. 2. The acoustic transmission spectra of Figs. 2(a) and 2(b) clearly show a strong attenuation extending from 192 to 312 kHz and from 400 to 487 kHz in the ΓX direction, and from 260 to 348 kHz in the ΓM direction. Overlapping these transmission spectra we find that a full band gap exists between 260 and 312 kHz when the two directions are considered jointly. In Fig. 2, the computed

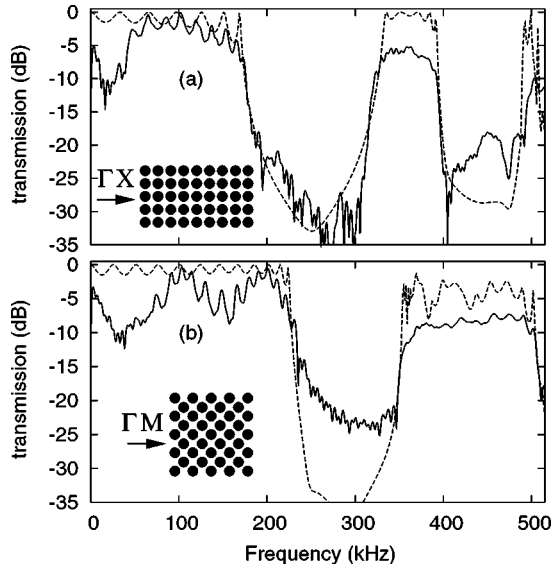

FIG. 2. Experimental (solid lines) and calculated (dashed lines) transmission power spectra along (a) the "ΓX" and (b) the "ΓM" directions of the irreducible Brillouin zone of the square lattice of steel cylinders in water. A full band gap extending from 260 to 312 kHz is obtained. The insets show the two-dimensional cross section of the ultrasonic crystal.

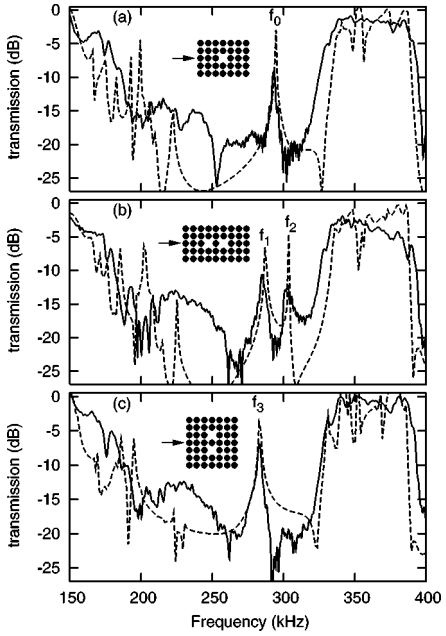

FIG. 3. Experimental (solid lines) and calculated (dashed lines) transmission power spectra vs frequency for interacting defects. (a) With one cylinder removed from the otherwise perfect crystal, a single defect induces a resonance mode in the stop band with frequency f_0. (b) Two defects in line with the incident wave induce two split resonance modes at frequencies f_1 and f_2 with an intercavity distance equal to one period. (c) Two defects are aligned perpendicularly to the incident wave.

FDTD transmission spectra are also presented. The location and the width of the band gaps in both directions of propagation compare very well with those observed experimentally. The FDTD transmission spectra were obtained numerically by discretizing time and space and replacing derivatives by finite differences in the elastic equation. The FDTD grids are composed of three adjacent regions, i.e., a central region containing the finite phononic crystal sandwiched between two homogeneous water regions. A traveling wave packet is launched in the first homogeneous region and propagates along the *Y* direction. Periodic boundary conditions are applied along the *X* direction and absorbing Mur's boundary conditions are imposed at the free ends of the homogeneous regions along the *Y* direction. The spectrum of the incoming signal is a Gaussian function with a full width at half maximum bandwidth of 1 GHz. The Fourier transform of this signal is also a Gaussian function and hence has smooth variations. The numerical transmission is obtained by averaging the displacement field at the end of the sample region along the *X* direction. This two-dimensional model is not supposed to account exactly for the experimental setup but should however catch its essential features.

Defective unit cells were then created by removing a single rod from the perfect crystal. This is expected to result in a localized defect mode within the acoustic band gap which is analogous to defect photonic modes[8] and acceptor impurity states in semiconductor physics.[9] The transmission through a crystal with a single defective unit cell was first measured and is shown in Fig. 3(a). The defect mode occurs

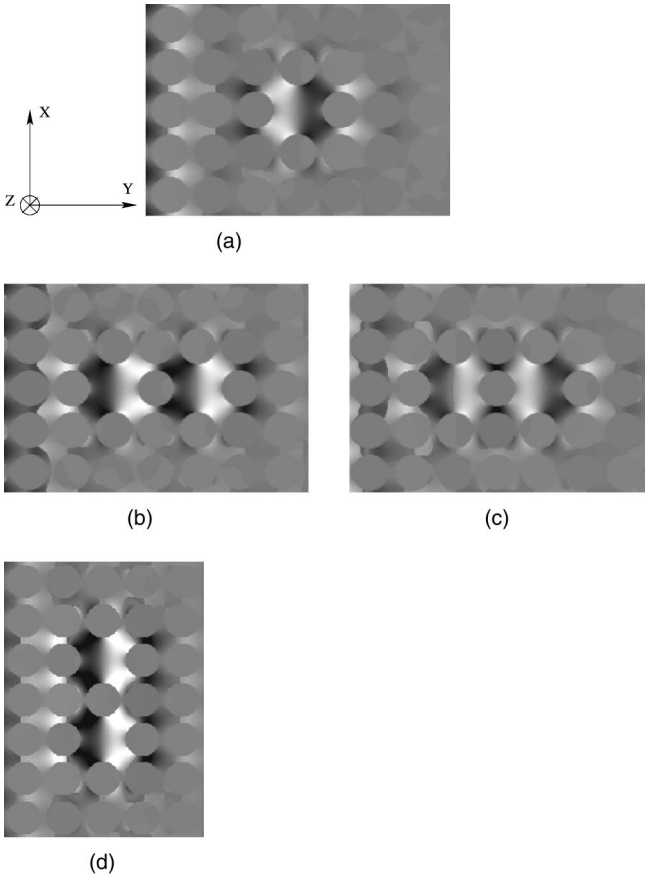

FIG. 4. The calculated longitudinal displacement amplitude averaged over one period of oscillation is shown at the resonance frequencies of defect modes indicated in Fig. 3. The incident wave is a longitudinal monochromatic plane wave propagating along axis *Y*. The single defect mode of Fig. 3(a) is visualized at frequency (a) $f_0=287.7$ kHz. The two double defect modes of Fig. 3(b) are visualized at frequencies (b) $f_1=280.0$ kHz and (c) $f_2=296.5$ kHz, respectively. The single defect mode of Fig. 3(c) is visualized at ferequency (d) $f_3=279.3$ kHz. Gray levels are representative of the amplitude and range from black for negative values to white for positive values. The positive and negative signs are inferred by keeping the instantaneous sign of the signal at every point in the space.

at a resonance frequency $f_0=287.7$ kHz. The transmission through the crystal was next measured with two consecutive rods removed along the *Y* direction, i.e., along the direction of propagation, and is shown in Fig. 3(b). It is observed that the localized mode of a single missing rod splits into two resonance modes with resonance frequencies $f_1=280$ and $f_2=296.5$ kHz, respectively. The intercavity distance for this case was 3 mm, which corresponds to a single period in the stacking direction. The effect of changing the separation between the cavities was also investigated both theoretically and experimentally. We found that the effect of the coupling between the two defects could be observed as far as the cavities are separated by less than four cylinders, with the frequency splitting decreasing to zero with distance. For longer separations, the transmitted signal becomes too small to be detected experimentally. Our interpretation is that de-

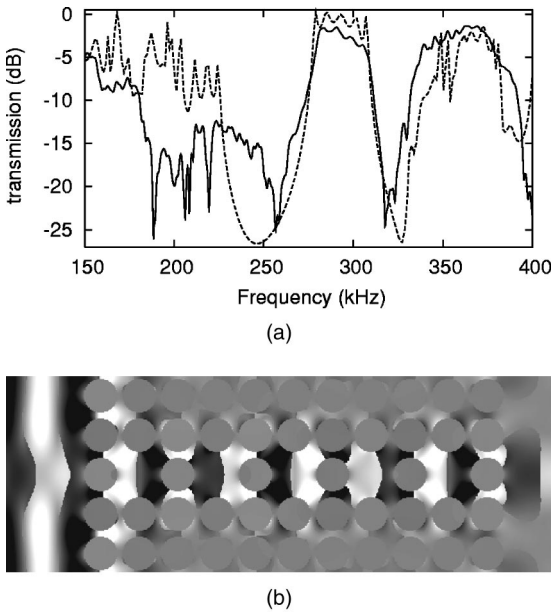

FIG. 5. (a) Experimental (solid line) and calculated (dashed line) transmission power spectrum vs frequency for five consecutive defects, along the propagation direction separated by one period in a 11 unit phononic crystal acting as a waveguide. (b) Calculated longitudinal displacement amplitude averaged over one period of oscillation. The incident wave is a longitudinal monochromatic plane wave with a 290 kHz frequency. The figure demonstrates the confinement and the guiding of the incident wave along the defect line.

fect modes are localized within the full band gap since their radiation is forbidden to enter the surrounding phononic crystal. Hence the coupling between defect modes is evanescent and the coupling strength decreases rapidly with their separation.

Since the cavity possesses two perpendicular mirror symmetry planes perpendicular to the *X* and the *Y* axis respectively, its eigenmodes can be labeled according to their symmetry with respect to these axes. We report in Fig. 4 the maps of the eigenvectors of cavity modes; these maps are obtained by considering an incident harmonic probing signal at the resonance frequencies in the transmission spectrum of Figs. 3(a) and 3(b). From these maps, one can notice that the eigenvector for a single defect is symmetrical with respect to both the *X* and the *Y* axes and that it is localized within the defect region. The modes of the pair of coupled cavities of Fig. 3(b) are still symmetrical with respect to the *Y* axis. However, each composite mode must be respectively antisymmetrical or symmetrical with respect to the mirror plane that separates the two cavities, i.e., the *X* axis. This is confirmed by visually inspecting the eigenvectors.

Figure 3(c) shows the transmission of a crystal having two coupled cavities oriented perpendicularly to the *Y* axis. In this geometry, the modes of the coupled cavities and their symmetries are the same as in the case of Fig. 3(b) but with the *X* and *Y* axes interchanged. Although two distinct modes are expected, only one is apparent, at the resonance frequency $f_3=279.3$ kHz. Indeed, due to the longitudinal polarization in water, the mode that is antisymmetrical with

respect to the Y axis cannot be excited. However, the mode at the resonance frequency f_3 is symmetrical with respect to the Y axis and can be excited by the incident probe wave. Its eigenvector [Fig. 4(d)] is essentially identical to that shown in Fig. 4(b) but with the X and Y axes interchanged.

When the number of defective unit cells is increased, a waveguiding band is expected to be formed due to the coupling of individual resonant modes. The transmission measured through a 11 unit-cell phononic crystal with five consecutive defects along the propagation direction, separated by one period, is shown in Fig. 5. The waveguiding band stands within the full acoustic band gap with a bandwidth $\Delta f = 42.5$ kHz. Nearly 100% transmission is observed throughout the waveguiding band. The FDTD calculation shows a good agreement with the measurements. In order to illustrate more clearly the confinement and the guiding of waves along the defects line, the field amplitude averaged over one period of oscillation is depicted in Fig. 5(b). This quantity gives a qualitative picture of the average energy distribution which is confined along the waveguide with no energy leaking out of the waveguide. The guiding mechanism originates from the evanescent coupling of the defect modes. This effect is a classical analog of quantum resonant tunneling. Qualitatively similar observations have been made in photonic crystals in the microwave regime.[8] Let us notice that the bandwith in Fig. 5(a) decreases significatly when increasing the intercavity separation, in the same way does the distance beteween the two peaks in Fig. 3(b). For an intercavity separation of two periods instead of one, the bandwith decreases from 42 kHz to 15 kHz.

In conclusion, we have investigated experimentally and theoretically the propagation of acoustic waves in the binary two-dimensional phononic crystal constituted by a square array of circular parallel steel cylinders in water. The measurements and the numerical calculations prove unambiguously the existence of an absolute stop band independent of the direction of propagation of the acoustic waves. We have observed that by removing a single rod from an otherwise perfect crystal, we could create a highly localized cavity or defect mode within the acoustic band gap. We have also shown the splitting of coupled localized cavity modes. This effect has been used as the basis for guiding acoustic waves within the stop band along a line of defects. An excellent agreement between experiment and theory was observed. To our knowledge, these are the first reported measurements of localized defects modes in two-dimensional phononic crystal, their resonance frequency splitting and the subsequent waveguiding effect.

We acknowledge fruitful discussions with Marc Solal and are grateful to Rabah Laihem for experimental assistance.

[1] M.M. Sigalas and E.N. Economou, Solid State Commun. **86**, 141 (1993).
[2] M.S. Kushwaha, P. Halevi, L. Dobrzynski, and B. Djafari-Rouhani, Phys. Rev. Lett. **71**, 2022 (1993).
[3] J.O. Vasseur, B. Djafari-Rouhani, L. Dobrzynski, M.S. Kushwaha, and P. Halevi, J. Phys.: Condens. Matter **6**, 8759 (1994).
[4] F.R. Montero de Espinosa, E. Jimenez, and M. Torres, Phys. Rev. Lett. **80**, 1208 (1998).
[5] V. Sanchez-Perez, D. Caballero, R. Martinez-Sala, C. Rubio, J. Sanchez-Dehesa, F. Meseguer, J. Llinares, and F. Galves, Phys. Rev. Lett. **80**, 5325 (1998).
[6] M.M. Sigalas and N. Garcia, J. Appl. Phys. **87**, 3122 (2000).
[7] J.O. Vasseur, P.A. Deymier, B. Chenni, B. Djafari-Rouhani, L. Dobrzynski, and D. Prevost, Phys. Rev. Lett. **86**, 3012 (2001).
[8] M. Bayindir, B. Temelkuran, and E. Ozbay, Phys. Rev. Lett. **84**, 2140 (2000).
[9] E. Yablonovitch, T.J. Gmitter, R.D. Meade, A.M. Rappe, K.D. Brommer, and J.D. Joannopoulos, Phys. Rev. Lett. **67**, 3380 (1991).
[10] A. Khelif, B. Djafari-Rouhani, J.O. Vasseur, P.A. Deymier, P. Lambin, and L. Dobrzynski, Phys. Rev. B **65**, 174308 (2002).
[11] M. Kafesaki, M.M. Sigalas, and N. Garcia, Phys. Rev. Lett. **85**, 4044 (2000).
[12] A. Khelif, B. Djafari-Rouhani, J.O. Vasseur, and P.A. Deymier, Phys. Rev. B **68**, 024302 (2003).
[13] M. Torres, F.R. Montero de Espinosa, D. Garcia-Pablos, and N. Garcia, Phys. Rev. Lett. **82**, 3054 (1999).
[14] F. Cervera, L. Sanchis, J.V. Sanchez-Perez, R. Martinez-Sala, C. Rubio, F. Meseguer, C. Lopez, D. Caballero, and J. Sanchez-Dehesa, Phys. Rev. Lett. **88**, 023902 (2002).
[15] S. Yang, J.H. Page, Z. Liu, M.L. Cowan, C.T. Chan, and P. Sheng, Phys. Rev. Lett. **88**, 104301 (2002).